This is the peer reviewed author accepted manuscript (post print) version of a published work that appeared in final form in:

Meng, Qingshi, Wu, Hao, Zhao, Zhiheng, Araby, Sherif, Lu, Shaowei, Ma, Jun 2017 'Free-standing, flexible, electrically conductive epoxy/graphene composite films', Composites part A: Applied science and manufacturing, vol. 92, pp. 42-50

This output may not exactly replicate the final published authoritative version for which the publisher owns copyright. It is not the copy of record. This output may be used for non-commercial purposes. This version is licensed under a Creative Commons CC-BY-NC-ND 4.0 license (http://creativecommons.org/licenses/by-nc-nd/4.0/).

The final definitive published version (version of record) is available at: 10.1016/j.compositesa.2016.10.028

Persistent link to the UniSA Research Outputs Repository: 11541.2/124501

General Rights

Copyright and moral rights for the publications made accessible in the UniSA Research Outputs Repository are retained by the authors and/or other copyright owners and it is a condition of accessing publications that users recognize and abide by the legal requirements associated with these rights.

- Users may download and print one copy for the purpose of private study or research.
- You may not further distribute the material or use it for any profit-making activity or commercial gain
- You may freely distribute the persistent link identifying the publication in the UniSA Research Outputs Repository

If you believe that this document breaches copyright, please contact us and provide details. We will remove access to the work immediately and investigate your claim.

Free-standing, flexible, electrically conductive epoxy/graphene composite films

Qingshi Meng [1], Hao Wu [2], Zhiheng Zhao [2], Sherif Araby [2, 3], Shaowei Lu[1], Jun Ma [*1, 2]

[1]Faculty of Aerospace Engineering, Shenyang Aerospace University, Shenyang, 110136, China
[2]School of Engineering, University of South Australia, Mawson lakes, SA, 5095, Australia
[3]Department of Mechanical Engineering, Faculty of Engineering, Benha University, Egypt

Abstract: Cost-effective, solution-processable and high-quality nanomaterials have critical roles in the development of advanced polymer composite films which combine mechanical robustness with functional properties such as electrical conductivity for many applications. This study first fabricated 3 nm-thick graphene platelets (GnPs) which have an electrical conductivity of 1460 S/cm; each platelet may contain double or a few layers of graphene whose C/O ratio was measured as 13.2. We then developed epoxy/GnP composite films by a layer-by-layer method through two-step curing. A percolation threshold of electrical conductivity was observed at merely 0.6 vol% GnPs, and the composite electrical conductivity increased to 1298.7 S/cm at 20.0 vol%. The composite films were mechanically strong to be used as the cost-effective electrodes for flexible supercapacitors. Specific capacitance 50.1 F/g was recorded for the 15.0 vol% composite film by two-electrode configuration, in comparison with the specific capacitance 41 F/g for commercial multi-walled carbon nanotubes. More importantly, impressive capacitance was found at a high current density of 20 A/g, which is desired in practical applications. The film electrode demonstrated a capacitance retention rate of 94.7% through 20,000 cycles. At a bending angle of 90°, it exhibited a capacitance of 38.9 F/g at 100 mV•s.

1. Introduction

Deformable, electrically conductive composite films are ubiquitous in numerous technological applications, and they constitute an ongoing topic of tremendous commercial interests. The polymers used in electronic industry are insulating, where static charge accumulates leading to potential damages due to catastrophic discharge. A substantial amount of research has been carried out to develop conductive polymer composites [1-6]; of all the fabrication methods developed, the addition of conductive fillers into polymeric matrices is the most cost-effective, which not only induces conductivity but may improve the mechanical properties such as stiffness.

The major challenge for polymer nanocomposites is the agglomeration of nanoparticles and the stacking of nanosheets at relatively low volume fractions (such as 3.0 vol%) due to phase separation [7], markedly reducing the effect of the dispersion phase on the composite functional and mechanical performance. Although the filler surface modification can prevent the agglomeration to a more or less extent, it inevitably coats a layer of organic molecules, leading to reduction or even loss of electrical conductivity. Therefore, it would be highly desirable to develop an effective approach to use un-modified nanomaterials and industrial materials such as epoxy resins for the development of composite films with high nanofiller fractions such as over 5.0 vol%. However, it remains a formidable challenge to prepare such high-fraction composites [8].

Traditional conductive fillers for polymers are made of either metals (such as stainless steel fibres) or noble metals (silver wires), reaching the limits of performance and conductive management applications. Metals are typically high-density materials adding undesirable weight to the composites; by contrast, the recently developed conductive nanocarbons have high conductivity and are not only light-weight but cost-effective. As a result, we herein advocate to develop electrically conductive polymer composites using carbon nanomaterials due to their relatively low density (~2.2g/cm^3) and very high thermal and electrical conductivity (up to ~3000 W/m-K and ~7200 S/m) [9].

Graphene sheets as conductive fillers are well-known for functionalizing and reinforcing polymers; in many cases graphene oxide or reduced graphene oxide was used. Graphene platelets (GnPs) of ~3 nm in thickness have been developed by thermally expanding a commercial graphite intercalation compound and subsequently ultrasonicating the expanded product [7]. GnPs have the following advantages in comparison with graphene oxide and reduced graphene oxide: (a) low defect concentration linking to a high electrical conductivity of 1460 S/cm [10], which implies no reduction

needed, (b) each platelet being ~3 nm in thickness, offering sufficient interface for stress and electron transfer in composites, and (c) cost-effectiveness (~$20/kg). These nanoscale GnPs have great potential to be used as fillers in materials for fabrication of electrically conductive composite films.

However, a glance at the literature shows no study performed to develop flexible epoxy films of high electrical conductivity using high-structural integrity graphene. This article presents a facile approach to the fabrication of composites films using a new layer-by-layer curing method which allows high fractions of graphene sheets dispersed in an epoxy matrix. The films demonstrate high performance as the electrodes for flexible supercapacitors.

2. Experimental

2.1 Materials

The graphite intercalation compound (GIC, Asbury 3494) and graphite powder (Micro 850) were supplied by Asbury Carbons, Asbury, NJ, USA. N-methyl-2-pyrrolidone (NMP), tetrahydrofuran (THF) and tri-isopropanolamine (TIPA) were ordered from Sigma Aldrich. Jeffamine D-400 (J400) and epoxy – diglycidyl ether of bisphenol A (Araldite-F, 182–196 g per equiv., denoted DGEBA) – were ordered from Huntsman Australia.

2.2 Fabrication of graphene platelets

Graphene platelets (GnPs) were prepared by a published method [7]. Briefly, a crucible was preheated in a furnace at 700°C for 5 min; 0.1 g GIC was transferred into the crucible and treated for one min, which is known as thermal shock. When the expanded product was cooled, it was suspended in acetone, followed by ultrasonication for two hours below 20°C, as low temperature promoted the exfoliation [11]. This produced GnPs.

2.3 Fabrication of epoxy/graphene composite film

Fig. 1 shows a schematic for the fabrication of epoxy/GnP composite films using a layer-by-layer method; the method comprising two curing steps is highly effective, while previous layer-by-layer methods do not work in this case since they have only one-step heat treatment [12-16]. GnPs were suspended at 0.1 wt% in acetone in a covered metal container by stirring with a magnetic bar for 10 min. An ultrasonic bath was used to treat the container for 30 min below 20°C, to suspend GnPs. DGEBA was added into the mixture by magnetically stirring for 10 min to reach dissolution, and then we added hardener–J400, followed by sonication under 20°C for 30 min. After sonication, half amount of acetone was evaporated at 50°C using a mechanical mixer; for suspensions with high graphene fractions, vacuum-oven degassing at room temperature (RT) was used to remove bubbles. The mixture was then dropped into a polypropylene mould by using a pipette. The remaining mixture was further evaporated and slightly cured at RT for 4 h to form a film. This process may repeat a few times to form a composite film of 0.2–0.4 mm in thickness. The film was finally cured in oven at 120°C for 12 hours.

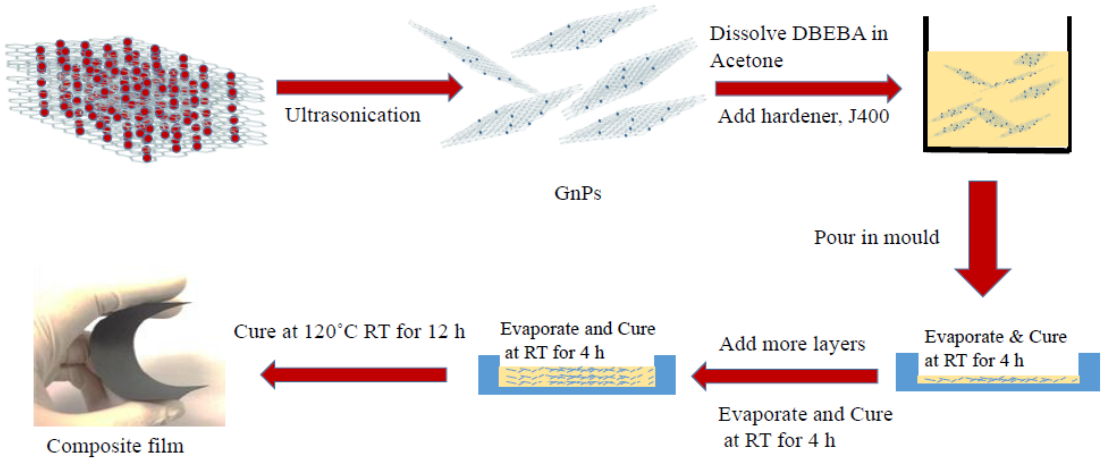


Fig. 1 Schematic for fabrication of epoxy/GnP composite films

2.4 Characterizations

GnPs were examined by AFM using a NT-MDT NTEGRA SPM instrument with NSG03 non-contact "golden" cantilevers. The oscillation magnitude was set as 15 nm and the scan rate for 2 × 2 μm images was at 0.5 Hz. GnPs were suspended at 0.0004 wt% in NMP by ultrasonication of 30 min below 30°C, and then the mixture was dropped on a silicon wafer and dried. We used a 100 μm scanner calibrated by 1.5 μm grids with 22 nm in height.

Transmission electron microscopy (TEM) micrographs were taken from a Philips CM200 at 200 kV. We prepared the samples by suspending GnPs in THF at 0.0004 wt% by 0.5-hour sonication and then dropped the suspension on 200-mesh copper grids, and dried.

GnPs and their composites were examined by X-ray diffraction (XRD) with a Diffraction Technology Mini-Materials Analyser (MMA), which had a diffractometer equipped with curved graphite monochromators and tuned to Cu Kα radiation (λ: 1.5419 Å). The spectra were collected within 2θ = 2–50° at 1 °/min.

Using a bench top press, GnP powder was pressed to create a sheet of less than 0.5 mm in thickness. A digital micrometre was used to measure the sheet thickness. The electrical conductivity was investigated by a Hall Effect measurement system having four probes. The probes were positioned with intimate surface contact with each sample, accurately at the four points of a square. Four current-

voltage graphs were made first to ensure intimate contact, and then resistivity testing was undertaken. Electrical conductivity was calculated based on the thickness. The composites containing high fractions of GnPs were similarly measured for conductivity.

Tensile testing and Young's moduli were performed at 0.5 mm/min at room temperature using an Instron 5567. Each set of data was obtained by using at least five specimens.

The through-plane electrical conductivity of the composites with low fractions of GnPs was measured using an Agilent 4339B high-resistivity meter connected with a 16008B resistivity cell at 25 °C. The testing was conducted in accordance with ASTM D257-99, and an average was made using over three measurements. Each sample is 5 ± 1.1 mm in thickness and 26 ± 0.5 mm in diameter.

The electrochemical characterization was undertaken by an electrochemical impedance spectroscopy (EIS, on a CHI 660E potentiostat, CH Instruments, Inc.) using 6 M KOH aqueous electrolyte with a two-electrode configuration. The electrodes were prepared by two symmetrical epoxy/GnP composite films with different ratios (5.0, 10.0 and 15.0 vol%). Two pieces of platinum sheets were used as the current collectors. The mass loading of one electrode was about ~5 mg. The capacitive performance of samples was characterized by using cyclic voltammetry (CV) and galvanostatic charge-discharge (GCD) techniques. The specific gravimetric capacitance of the working electrode, C (in F/g), was obtained from the discharge curve according to the following equation:

The specific capacitance (C2, F/g) was calculated from both cyclic voltammetry and charge-discharge graphs according to following equation (1) and (2), respectively [17, 18]:

$$\mathbf{C_2} = \frac{4\int_{V_1}^{V_n} i\,dV}{mv\,\Delta V} \qquad (1)$$

$$\mathbf{C_2} = \frac{4I\,\Delta t}{m\,\Delta V} \qquad (2)$$

Where $\int_{V_1}^{V_n} i\,dV$ is the integrated value of the cyclic voltammetry graph, m is the total mass of the active materials in both electrodes, v is the scan rate (V/s), Δt is the discharging time, I is the current applied on the electrodes, and ΔV is the potential window of the discharging process.

3. Results and discussion

3.1 Characterization of graphene platelets (GnPs)

By randomly picking up 20 sheets, the thickness was measured as 3.51 ± 0.37 nm by AFM, with one representative measurement shown in Fig. 2. Since thermal expansion was reported to produce a graphene sheet of ~1 nm in thickness [19], each GnP produced in this study may contain 2-4 graphene sheets. *GnPs are different to graphite nanosheets and nanoplatelets, in that the latter are far thicker than 5 nm. A theoretical model (please see Figure 3 in Ref [20]) shows that the sheets of below 5 nm in thickness can have far more interface area than those of over 5 nm in thickness. This means that thin GnPs can have far more reinforcing and toughening effects than graphite nanosheets.*

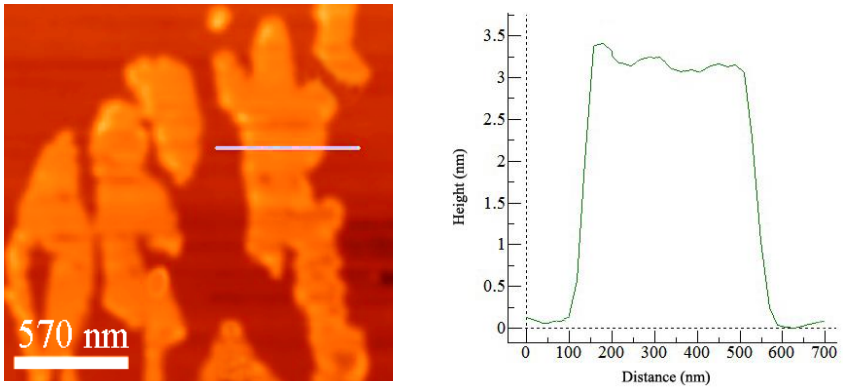


Fig. 2 AFM images and height measurement of typical graphene platelets

Fig. 3a shows the representative morphology of GnPs. Pieces of sheets are found sitting on lacey carbon support, clearly illustrating flake-like structure. Fig. 3b exhibits a high magnification TEM image of a randomly selected area of the platelets without lacey-carbon support. There were some overlapped structures located at the right side of the image (see black arrows). The most transparent and featureless region (orange arrows in Fig. 3b) likely possesses ultra-thin crystal structure, where we randomly selected a point to examine the electron diffraction (ED) pattern. The pattern in Fig. 3c shows a typical six-fold symmetry expected for highly crystalline structure, and its diffraction in Fig. 3d illustrates a stronger outer intensity than inner ($I_{1\text{-}210}/I_{0\text{-}110}$ is greater than 1), confirming that the region contains 2-3 layers of graphene sheets [21, 22]. The investigation is in agreement with our AFM measurement.

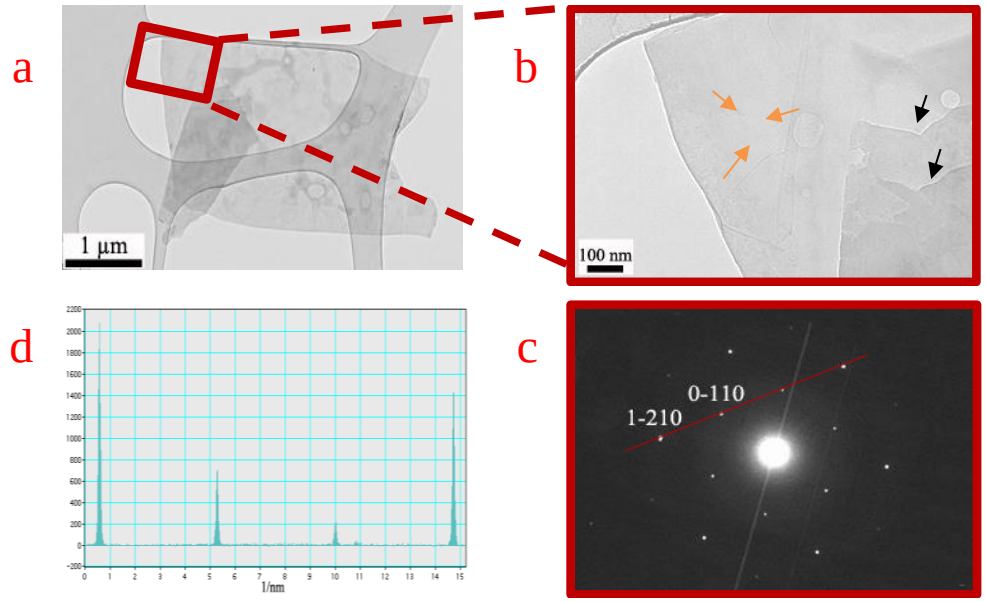


Fig. 3 Morphology of GnPs: (a) and (b) TEM images, (c) electron diffraction pattern taken from (b) where the peaks labelled by Miller-Bravais indices, and (d) diffraction intensity taken along the 1–210 to 0-110 axis, corresponding to double- or triple-layer graphene.

The high crystalline structure of GnPs is in agreement with the XPS analysis (Fig. 1a of the data in brief) which shows a *C/O* ratio of 13.2. Thus, our GnPs would be a promising precursor for the fabrication of highly conductive composite films. Fig.1b of the data in brief contains FT-IR spectra of GnPs. Our GnPs contain sufficient functional groups for either chemical modification or promoting their dispersion in solvents.

In data in brief Fig. 2, GnPs demonstrate obvious absorptions at 1339, 1586 and 2695 cm^{-1} which correspond to D, G, and 2D bands, respectively. G band relates to sp^2 resonance on an ordered graphitic lattice, while D band is activated from the first-order scattering process of sp^2 carbons by the presence of in-plane substitutional hetero-atoms, vacancies, grain boundaries or other defects, which might be sp^3 hybridized carbon structure associating with impurity or oxidation degree. Since all samples were tested in the form of powder, there is no point to discuss 2D band. The D- to G-band ratio of GnPs (I_D/I_G = 0.068) is far smaller than those of reduced graphene oxide (~1) and GIC (0.57) [23, 24], revealing a far better structural integrity. This conclusion aligns with our TEM and XPS analysis.

3.2 Characterization of epoxy/GnP composite film

3.2.1 Electrical properties

Polymeric materials having electrical conductivity over 10^{-9} S/cm are recognized as a semi-conductive material in engineering applications, while an electrical conductivity of about 10^{-6} S/cm is sufficient for anti-static applications [25]. Since epoxy resins are extensively used in aerospace and electronics industries, it is of significance to manipulate their electrical resistance/conductivity by using conductive nanomaterials [10, 25-28]. The electrical properties of polymer composites mainly depend on the filler conductivity, geometry, fractions, dispersion and interaction with matrices. Since the high-electrical conductivity GnPs adopted in this study have a number of surface functional groups such as epoxide groups which help to suspend in solvent, no further modification was made so as to minimize surface defects. Hence the dispersion and fraction of GnPs are crucial to determine the final electrical properties of epoxy composites.

Through-plane electrical conductivity for composites having low GnP fractions: Generally, through-plane electrical conductivity (volume resistivity) is designed for insulating or semi-conductive materials, which we thus used for epoxy films containing low fractions of GnPs. In Fig. 4a, the neat epoxy conductivity increases by orders of magnitude upon compounding with GnPs. At 2.3 vol%, the conductivity improves from 10^{-15} to 10^{-6} S/cm. By fitting experimental data into the power law equation, we obtained a percolation threshold (the formation of pathways for electron transfer) of 0.6 vol %, as shown in the bottom right corner of Fig. 4a. It is worth noting that the composite film threshold is lower than those in previous studies [7, 10] likely because a longer period of sonication (1 hour in total) was used in the composite preparation. *When these thin films were made layer by layer, GnPs more likely align and orient themselves in the film plane, which contributed much to the low percolation threshold.*

In-plane electrical conductivity for composites with high filler fractions: Since the four-probe method is usually used for conductive materials, it was used in this study to measure the composites have higher fractions of GnPs. As shown in Fig. 4b, the average sheet resistance of films is at 1201 – 7.7 Ω/square (red curve), corresponding to electrical conductivity from 8.3 to 1298.7 S/cm. The epoxy/GnP composite film shows an electrical conductivity of 1298.7 S/cm at 20.0 vol%, much higher than those of the films made from neat graphene oxide with tedious chemical or electrochemical reduction [29]; this is because the electrical conductivity of our GnPs is much higher than that of GnO as well as reduced GnO. Notably, our GnPs were prepared by a simple thermo-sonication method where reduction is not needed due to their high structural integrity (see Fig.1a of the data in brief).

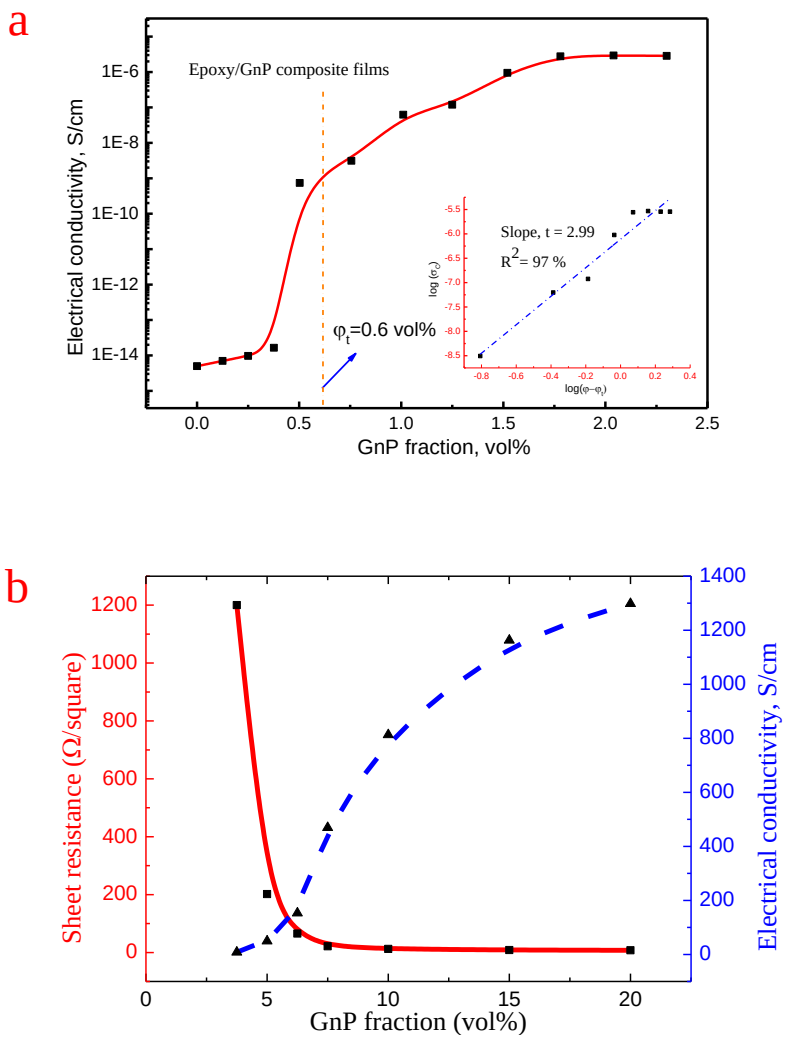


Fig.4 (a) Through-plane electrical conductivity of epoxy/GnP composite films at low volume fractions and (b) sheet resistance and electrical conductivity of epoxy graphene films at high fractions.

3.2.2 Mechanical performance

Since our composite films at high GnP fractions demonstrate high electrical conductivity, it is worth to particularly investigate the mechanical performance of these films for a potential wide range of applications. For composites having relatively ductile matrices, tensile strength can be improved by introducing inorganic nanosheets [30-35]. *But tensile strength is often reduced in rigid matrices such as brittle epoxy resins and PMMA [23, 36-39]. These reductions are mainly caused by relatively poor interfacial bonding between GnPs and epoxy matrix in comparison with the dense crosslinking network.* At 5.0, 10.0 and 15.0 vol% GnPs, the composite films show tensile strength at 9.6, 7.0 and 3.6 MPa respectively (Fig. 5); the reduction was explained below.

The conventional one-step curing method failed in the fabrication of epoxy films containing a high loading of GnPs such as 5.0 vol%. Thus we developed a layer-by-layer curing method, where each layer was partially cured at room temperature (see experimental section); the curing would lock each platelet in the layer effectively preventing the platelets from stacking. At the percolation threshold of electrical conductivity, GnPs start to form networks; with increase in the fractions, more platelets would contact each other physically whilst epoxy resin may form more island-like structure.

In a conventional two-phase polymer blend, both dispersion phase and matrix are polymeric. A two-continuous phase composite would form with increase in the dispersion phase fraction. With further increase, the matrix may become the dispersion phase, depending on the compatibility, viscosity match and volume fraction. But in this work GnPs are the dispersion phase. There will be less volume fraction of epoxy with increase in GnP fractions. At high fractions, GnPs may contact with each other, and in some regions they would wrap epoxy forming island-like structure. In Fig 6c, GnPs are observed everywhere, which may help epoxy to form some island-like structure. Although this kind of structure reduces much tensile strength, it should pose no effect on the percolation threshold because it forms only at high GnP fractions.

This explains the obvious drop in tensile strength in Fig. 5. Nevertheless, these films would be sufficiently strong and deformable for applications such as supercapacitor electrodes, as to be discussed later.

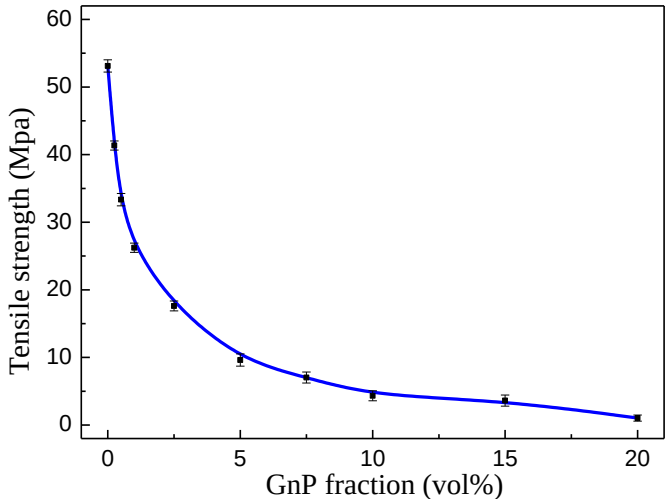


Fig. 5 Mechanical properties of epoxy/GnP composite films.

The stiffness (young's modulus) of the composite films containing low to high loading of GnPs (0–7.5 vol %) was measured (see Fig.3a in data in brief). The moduli of composite films increase with GnP fractions at a low loading range. A slightly knee-like feature is observed in Fig.3a of the data in brief, implying that the stiffening effect of GnPs on the matrix becomes less obvious with further increase in GnP fractions; this may represent a transition of morphology. The 2.5 vol% GnPs improved the Young's modulus of epoxy from 2620 ± 98 MPa to 3089 ± 88 MPa, 17.9% enhancement. At 5.0 vol% GnPs, the composite stiffness is only 3060± 98 MPa, followed by a further down at 7.5 vol%; the reduction should be caused by the porous structure, as detailed in the following morphological analysis.

3.3 Morphology of composite films

The neat epoxy film in general is featureless and has a relatively smooth cross-section surface structure (See Fig. 4 of the data in brief). By contrast, the epoxy/GnP composite films at a high filler fraction have layered, porous structure as shown in the cross-section SEM micrographs (Fig. 6). This type of structure is explained as below. The platelets would stack themselves with epoxy resins at high fractions. During this process, epoxy resin may be unable to completely fill the interlayer spacing, likely leaving interlayer channels. The stacked platelets would form particles, between which pores may exist. The increase in the GnP fractions would cause more interlayer channels and inter-particle pores. Since the high fraction composite films demonstrate decent mechanical robustness, high electrical conductivity and porous structures, we proceeded to investigate their specific capacitance.

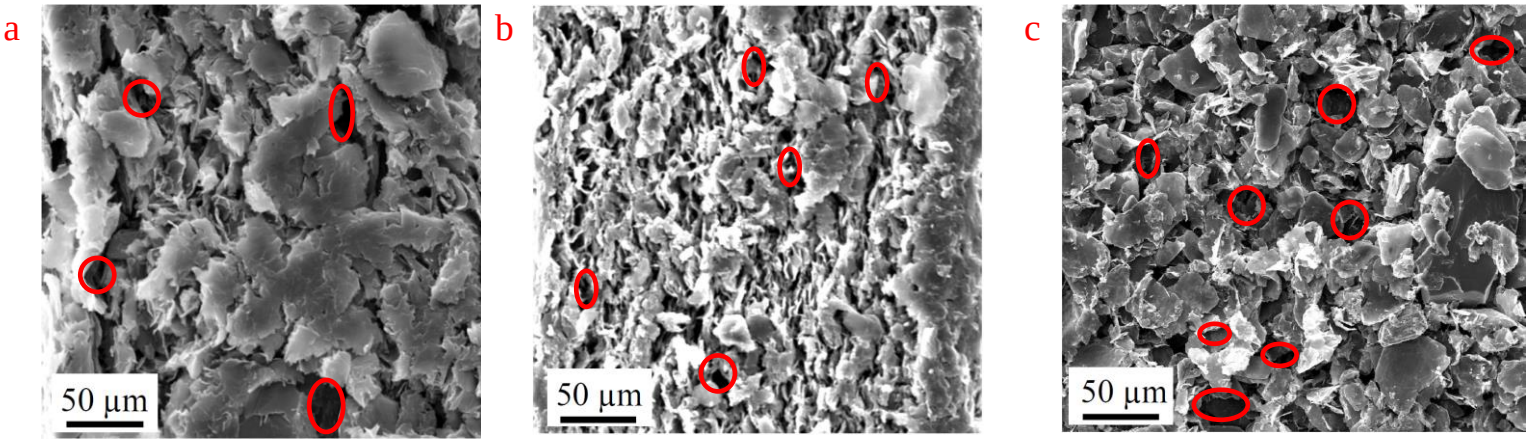


Fig. 6 SEM images of cross section of the epoxy/GnP films with layered and porous structures indicated by red circles. (a) 5.0 vol %, (b) 10.0 vol% and (c) 15.0 vol%.

3.4 Specific capacitance of conductive films as electrodes for supercapacitors

Since the composite films are electrically conductive and they are porous, we proceeded to use a piece of the film as the electrode material for supercapacitors; the active material is 1 × 1 cm^2 in lateral dimension having a density of ~0.4 g/cm^3. It was characterized by cyclic voltammetry (CV) and galvanostatic charge/discharge (GCD) technique with a two-electrode configuration.

Fig. 7a shows the CV graphs of the film electrodes in 6 M KOH electrolyte at a scan rate of 50 mV/s within 0 – 1 V. For neat epoxy, CV curve is a straight line, implying no electrochemical capacitance. In comparison, the composite films show a near rectangular shape, implying a relatively high current response for pseudocapacitance behaviour; this should be contributed by our GnPs which have a lot surface functional groups such as epoxide groups (Fig. 1b of the data in brief) and feature high electrical conductivity 1460 S/cm. *Therefore, the mechanisms of the supercapacitive performance can be classified as electrochemical double layer capacitances (EDLCs) and pseudocapacitances, both of which are derived from the hydroxide groups and high electrical conductivity of GnPs [40].*

The CV curve of the 15.0 vol% composite films is less rectangle than other two, but it has larger area representing the highest specific capacitance. The reason is that the high fraction composite films have more interlayer channels and inter-particle pores, which have more GnP functional groups involved in the redox reactions. Pseudocapacitance takes more important role in capacitance enhancement for the

15% composite film. The highly porous structure (Fig. 6c) between stacked sheets of the 15% film provides a sufficient number of sites to trap the ions, and it offers channels to transport the electrolyte for redox reactions of functional groups. The specific capacitance values calculated from CV curves are 15.0, 19.6 and 50.1 F/g, and volumetric capacitance 6.0, 7.8 and 20.0 F/cm^3, respectively for composite films containing 5.0 vol%, 10.0 vol% and 15.0 vol% GnPs. The increase in specific capacitance with GnP fractions is consistent with the electrical conductivity enhancement of epoxy/GnP composite films, because more GnPs create more electron pathways in the composites, leading to transfer of more electrons for EDLC and also more surface oxygen-containing groups for pseudocapacitance.

It is worth to compare the performance of our epoxy/GnP composites with that of the film where GnPs were replaced by graphite. In Fig.5 of the data in brief, the CV graph of the 15.0 vol% epoxy/graphite composite film is observed as a straight line implying nearly no electrochemical capacitance, which is nearly the same as neat epoxy. By contrast, the 15.0 vol% epoxy/graphene composite film shows a remarkable CV graph relating to a specific capacitance of 50.1 F/g. This phenomenon can be explained below. (i) Our GnPs have an electrical conductivity of 1460 S/cm, far higher than the electrical conductivity of graphite 1 S/cm. The 15.0 vol% epoxy/graphite composite film is mainly limited by a low electrical conductivity of 0.83 S/cm, whilst the 15.0 vol% epoxy/GnP composite film features 1162.8 S/cm. The low conductivity of the graphite composite seriously limits electron transportation to create capacitance. And (ii) graphite also has far less total particle surface area than GnPs which have many interlayer channels and pores to help create high capacitance. This is further explained by XRD measurement (Fig.7 and Table 1) in data in brief.

The capacitance of the 15.0 vol% epoxy/GnP composite film is also higher than commercial MWCNTs (41 F/g) and close to a MWCNT-graphene hybrid (71 F/g) [41]. Another advantage of our epoxy/GnP composite films is the robust mechanical performance (see the discussion in the section 3.2.2), enabling the films to be used as flexible electrodes for long service life.

Fig. 7b contains the galvanostatic charge/discharge (GCD) curves of the composite films tested at 0.2 A/g. With increase in GnP loading, these films show specific capacitance at 9.9, 14.9 and 30.6 F/g, and volume capacitance at 4.0, 6.0 and 11.5 F/cm^3. All these agree with the capacitance calculated from CV graphs. The GCD curves of 5.0 vol% and 10.0 vol% composite films are almost linear and symmetrically mirrored to its discharge counterparts, which indicates a perfect electrochemical capacitor behaviour. Similar to the CV curve, the unsymmetrical triangle sharp of GCD curve for 15.0 vol% composite film is caused by the redox reactions.

We specifically investigated the performance of the 15.0 vol% epoxy/GnP composite film at 50 – 500 mV/s. In Fig. 7c, the cyclic voltammetry (CV) curves display similar rectangular shapes at different scan rates. The specific capacitances calculated from the CV curves (Fig. 7c) are respectively 50.1, 43.0, 38.0 and 36.0 F/g as shown in Fig.6 of the data in brief. The specific capacitances calculated from the charge/discharge curves are respectively 30.6, 26.6, 25.0 and 23.3 F/g at different current density (from 0.2 to 2 A/g) in Fig. 7d, all of which are much higher than those of 10.0 vol% and 5.0 vol% composite films ranging from 14.9 to 7.8 F/g and from 9.9 to 4.6 F/g, respectively. The markable difference should be mainly caused by the difference in the electrical conductivity of these composites. The 15.0 vol% composite has an electrical conductivity of – 1162.8 S/cm, 43.0 % higher than those of the 10.0 vol% composite – 813.01 S/cm.

It is a formidable challenge for supercapacitors to attain satisfactory performance at an ultra-high current density such as 20 A/g. Since our composite films showed high electrical conductivity, we measured the electrochemical performance at a current density up to 20 A/g. In Fig. 7e, the discharge time decreases with increase in the current density, and the specific capacitance at 20 A/g was found to be 23.3 F/g, which is rather impressive in terms of costs and performance when compared with previous studies. It also shows a high capacitance retention rate of 76% when the current density increases from 0.2 to 20 A/g. Liang developed a porous graphene paper which had a capacitance retention of 62% at 0.2 – 20 A/g [42].

There might be two reasons for the high performance of the 15.0 vol% epoxy/GnP composite film. First, the film has a high conductivity of 1162.8 S/cm in comparison with the other two composite films. Second, more oxygen-containing groups of GnPs may help to absorb more electrolyte into the film, resulting in an enhanced interface between fillers and electrolyte. With increase in GnP fractions, more interlayer channels and inter-particle pores were found in epoxy/GnPs composite film, especially in the 15.0 vol% composite film (see discussion for the Morphology of composite films). As a result, more functional groups on GnPs surface were exposed to electrolyte. Pseudo-capacitance produces more efficient contribution to total capacitance at 15.0 vol% rather than that of 5.0 vol% and 10.0 vol%.

Therefore, the interface for 15.0 vol % epoxy/GnP composite film could feature the higher level of ion transferring ability.

The cyclic stability was measured for these composite film electrodes. The capacitance decay was examined by continuous GCD measurement between 0 to 1 V at 1 A/g for 20,000 cycles. Fig. 7f show

that capacity retentions are 94.7%, 89.2% and 84.3% respectively for the films at 15.0 vol%, 10.0 vol% and 5.0 vol%. *The first cycle shows a higher capacitance than others, because of the porous structure relating to large-area interface between electrodes and electrolytes and thus high capacitance. The porous structure evolved itself through the first few cycles to obtain a stable capacitance for the following cycles.* The long-term cycling testing shows high stability for all the samples, which would be caused by the high structural integrity of graphene and the mechanical robustness of the composite films. Therefore, our composite films have potential to be used as the electrodes for energy storage devices.

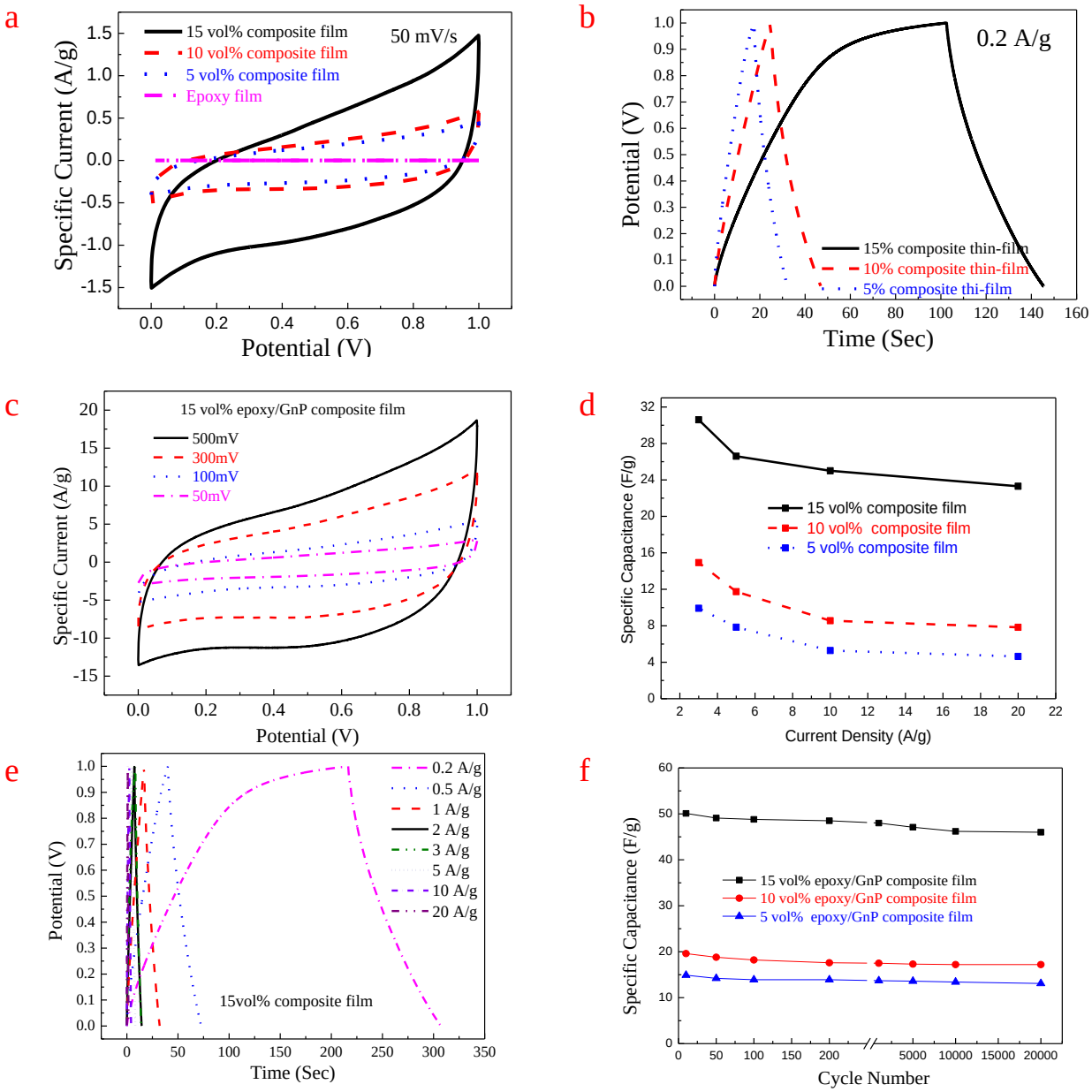


Fig. 7 Electrochemical characterization of supercapacitors based on epoxy composite films containing 15.0 vol%, 10.0 vol% and 5.0 vol% graphene platelets (GnPs): (a) CV curves obtained at 50 mV/s, (b) charge/discharage curves at 0.2 A/g, (c) CV curves at various scan rate, (d) specific capacitances, (e) CD curves of the 15.0 vol% composite film, and (f) cyclic stability.

3.5 Flexible supercapacitor

We utilized two pieces of indium tin oxide (ITO)-coated PET as the current collectors. We prepared solid electrolyte by mixing 20 ml 6 M KOH electrolyte with 2 g PVA at 85°C to obtain a transparent

mixture. Then the electrolyte was coated on the electrode, followed by drying at room temperature. We made layers of the electrolyte and the electrodes, and then interleaved these layers, followed by pressing guarantee intimate contact. This produced flexible supercapacitors.

The electrochemical performance of the 15.0 vol% epoxy/GnP composite films under different bending conditions is illustrated in Fig. 8. As shown in Fig. 8a, as-prepared supercapacitors (composite films) could be bent to 90˚, demonstrating good flexibility. The CV graphs in Fig, 8b *and 8c* demonstrate slightly variation with bending angles of 180˚, 120˚ and 90˚ which respectively correspond to 41.5, 40.1 and 38.9 F/g *at 100 mV/s or 28.9, 28.3, 27.5 F/g at 0.2 A/g*. It demonstrates that our composite films can be used to develop flexible supercapacitors.

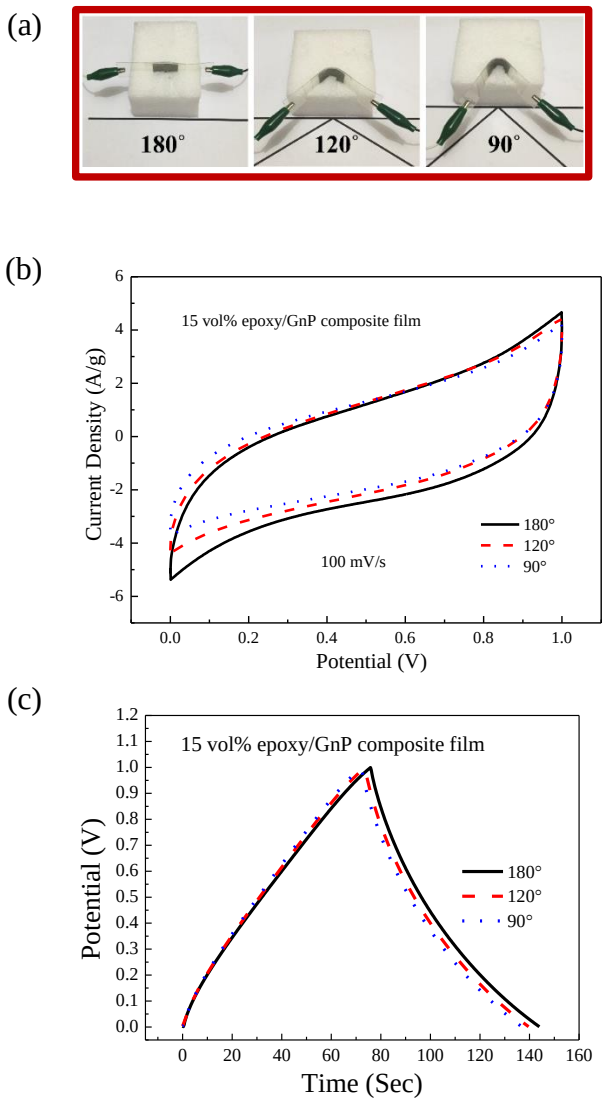


Fig. 8 A flexible supercapacitor with various (a) bending angles, and (b) corresponding CV curves *(c) charge/discharge curves*.

Conclusions

By using 3 nm-thick GnPs which have high structural integrity and can be processed in solution, we developed electrically conductive composite films by a layer-by-layer method through two-step curing. A percolation threshold of electrical conductivity was observed at merely 0.6 vol% GnPs, and the composite conductivity increased to 1298.7 S/cm at 20.0 vol%. The composite films at high GnP fractions are sufficiently robust to be used as electrodes for supercapacitors. Using two-electrode configuration, the 15.0 vol% composite film revealed a specific capacitance of 50.1 F/g higher than the capacitance 41.0 F/g for multi-walled carbon nanotubes. More importantly, it demonstrated high performance at a large current density of 20 A/g. The composite film can be used as a flexible supercapacitor. When bent at 90°, the 15% composite supercapacitor exhibited 38.9 F/g at 100 mV·s. It had 94.7% retention through 20,000 cycling measurement.

Acknowledgements

JM and QM thank Animesh Basak and Angus Netting for technical support at Adelaide Microscopy. JM thanks Asbury and Huntsman (Melbourne) for providing the graphite intercalation compound and J400 respectively. JM would like to acknowledge the support by an Australian Research Council Linkage project (LP160100717).

References：

[1] Hansen TS, West K, Hassager O, Larsen NB. Highly Stretchable and Conductive Polymer Material Made from Poly (3, 4 - ethylenedioxythiophene) and Polyurethane Elastomers. Advanced functional materials. 2007;17(16):3069-73.

[2] Chun K-Y, Oh Y, Rho J, Ahn J-H, Kim Y-J, Choi HR, et al. Highly conductive, printable and stretchable composite films of carbon nanotubes and silver. Nature nanotechnology. 2010;5(12):853-7.

[3] Park M, Park J, Jeong U. Design of conductive composite elastomers for stretchable electronics. Nano Today. 2014;9(2):244-60.

[4] Jia W, Tchoudakov R, Narkis M, Siegmann A. Performance of expanded graphite and expanded milled - graphite fillers in thermosetting resins. Polymer Composites. 2005;26(4):526-33.

[5] Zheng W, Wong SC. Electrical conductivity and dielectric properties of PMMA/expanded graphite composites. Composites Science & Technology. 2003;63(2):225-35.

[6] Li J, Man LS, Kim JK, Marom G. Morphology and properties of UV/ozone treated graphite nanoplatelet/epoxy nanocomposites. Composites Science & Technology. 2007;67(2):296-305.

[7] Zaman I, Kuan H-C, Dai J, Kawashima N, Michelmore A, Sovi A, et al. From carbon nanotubes and silicate layers to graphene platelets for polymer nanocomposites. Nanoscale. 2012;4(15):4578-86.

[8] Balandin AA. Thermal properties of graphene and nanostructured carbon materials. Nature materials. 2011;10(8):569-81.

[9] Kuilla T, Bhadra S, Yao D, Kim NH, Bose S, Lee JH. Recent advances in graphene based polymer composites. Progress in Polymer Science. 2010;35(11):1350-75.

[10] Meng Q, Jin J, Wang R, Kuan H-C, Ma J, Kawashima N, et al. Processable 3-nm thick graphene platelets of high electrical conductivity and their epoxy composites. Nanotechnology. 2014;25(12):125707.

[11] Zaman I, Phan TT, Kuan H-C, Meng Q, La LTB, Luong L, et al. Epoxy/graphene platelets nanocomposites with two levels of interface strength. Polymer. 2011;52(7):1603-11.

[12] Eda G, Chhowalla M. Graphene-based Composite Thin Films for Electronics. Nano Letters. 2009;9(2):814-8.

[13] Ramanathan T, Abdala A, Stankovich S, Dikin D, Herrera-Alonso M, Piner R, et al. Functionalized graphene sheets for polymer nanocomposites. Nature nanotechnology. 2008;3(6):327-31.

[14] Akhavan O. The effect of heat treatment on formation of graphene thin films from graphene oxide nanosheets. Carbon. 2010;48(2):509-19.

[15] Dai JB, Kuan HC, Du XS, Dai SC, Ma J. Development of a novel toughener for epoxy resins. Polymer International. 2009;58(7):838-45.

[16] Ma J, Qi Q, Bayley J, Du XS, Mo MS, Zhang LQ. Development of SENB toughness measurement for thermoset resins. Polymer Testing. 2007;26(4):445-50.

[17] Moussa M, Zhao Z, El-Kady MF, Liu H, Michelmore A, Kawashima N, et al. Free-standing composite hydrogel films for superior volumetric capacitance. Journal of Materials Chemistry A. 2015;3(30):15668-74.
[18] Zhao Z, Richardson GF, Meng Q, Zhu S, Kuan H-C, Ma J. PEDOT-based composites as electrode materials for supercapacitors. Nanotechnology. 2015;27(4):042001.
[19] Meyer JC, Geim AK, Katsnelson M, Novoselov K, Booth T, Roth S. The structure of suspended graphene sheets. Nature. 2007;446(7131):60-3.
[20] Araby S, Zaman I, Meng Q, Kawashima N, Michelmore A, Kuan HC, et al. Melt compounding with graphene to develop functional, high-performance elastomers. Nanotechnology. 2013;24(16):165601.
[21] Vallés C, Drummond C, Saadaoui H, Furtado CA, He M, Roubeau O, et al. Solutions of negatively charged graphene sheets and ribbons. Journal of the American Chemical Society. 2008;130(47):15802-4.
[22] Hernandez Y, Nicolosi V, Lotya M, Blighe FM, Sun Z, De S, et al. High-yield production of graphene by liquid-phase exfoliation of graphite. Nature nanotechnology. 2008;3(9):563-8.
[23] Ma J, Meng Q, Michelmore A, Kawashima N, Izzuddin Z, Bengtsson C, et al. Covalently bonded interfaces for polymer/graphene composites. Journal of Materials Chemistry A. 2013;1(13):4255.
[24] Zaman I, Kuan HC, Meng Q, Michelmore A, Kawashima N, Pitt T, et al. A facile approach to chemically modified graphene and its polymer nanocomposites. Advanced Functional Materials. 2012;22(13):2735-43.
[25] Ma P-C, Siddiqui NA, Marom G, Kim J-K. Dispersion and functionalization of carbon nanotubes for polymer-based nanocomposites: a review. Composites Part A: Applied Science and Manufacturing. 2010;41(10):1345-67.
[26] Li J, Ma PC, Chow WS, To CK, Tang BZ, Kim JK. Correlations between Percolation Threshold, Dispersion State, and Aspect Ratio of Carbon Nanotubes. Advanced Functional Materials. 2007;17(16):3207–15.
[27] Lu C, Mai YW. Influence of aspect ratio on barrier properties of polymer-clay nanocomposites. Physical Review Letters. 2005;95(8).
[28] Celzard A, Mcrae E, Deleuze C, Dufort M, Furdin G, Marêché JF. Critical concentration in percolating systems containing a high-aspect-ratio filler. Physical Review B Condensed Matter. 1996;53(10):6209-14.
[29] Parvez K, Li R, Puniredd SR, Hernandez Y, Hinkel F, Wang S, et al. Electrochemically exfoliated graphene as solution-processable, highly conductive electrodes for organic electronics. ACS nano. 2013;7(4):3598-606.
[30] Araby S, Zaman I, Meng Q, Kawashima N, Michelmore A, Kuan H-C, et al. Melt compounding with graphene to develop functional, high-performance elastomers. Nanotechnology. 2013;24(16):165601.
[31] Araby S, Meng Q, Zhang L, Kang H, Majewski P, Tang Y, et al. Electrically and thermally conductive elastomer/graphene nanocomposites by solution mixing. Polymer. 2014;55(1):201-10.
[32] Araby S, Meng Q, Zhang L, Zaman I, Majewski P, Ma J. Elastomeric composites based on carbon nanomaterials. Nanotechnology. 2015;26(11):112001.

[33] Meng QS, Wang CH, Saber N, Kuan HC, Dai JB, Friedrich K, et al. Nanosilica-toughened polymer adhesives. Materials & Design. 2014;61(0):75-86.

[34] Ma J, La LTB, Zaman I, Meng Q, Luong L, Ogilvie D, et al. Fabrication, Structure and Properties of Epoxy/Metal Nanocomposites. Macromolecular Materials & Engineering. 2011;296(5):465–74.

[35] Meng QS, Zaman I, Hannam JR, Kapota S, Luong L, Youssf O, et al. Improvement of adhesive toughness measurement. Polymer Testing. 2011;30(2):243-50.

[36] Ma J, Shi L, Yang M, Li B, Liu H, Xu J. Synthesis and structure of polymethylsilsesquioxane–clay nanocomposite via in situ intercalative polymerization. Journal of Applied Polymer Science. 2002;86(14):3708-11.

[37] Meng QS, Kuan HC, Araby S, Kawashima N, Saber N, Wang CH, et al. Effect of interface modification on PMMA/graphene nanocomposites. Journal of Materials Science. 2014;49(17):5838-49.

[38] Kuan HC, Dai JB, Ma J. A reactive polymer for toughening epoxy resin. Journal of Applied Polymer Science. 2010;115(6):3265–72.

[39] Li F, Lu Y, Li L, Zhang L, Dai J, Ma J. Relations between carbon nanotubes' length and their composites' mechanical and functional performance. Polymer. 2013;54(8):2158-65.

[40] Zhiheng Z, Georgia FR, Qingshi M, Shenmin Z, Hsu-Chiang K, Jun M. PEDOT-based composites as electrode materials for supercapacitors. Nanotechnology. 2016;27(4):042001.

[41] Odedairo T, Ma J, Gu Y, Chen J, Zhao X, Zhu Z. One-pot synthesis of carbon nanotube–graphene hybrids via syngas production. Journal of Materials Chemistry A. 2014;2(5):1418-28.

[42] Liang Q, Ye L, Huang Z-H, Xu Q, Bai Y, Kang F, et al. A honeycomb-like porous carbon derived from pomelo peel for use in high-performance supercapacitors. Nanoscale. 2014;6(22):13831-7.